Talanta 312 (2027) 130327

Contents lists available at ScienceDirect

Talanta

journal homepage: www.elsevier.com/locate/talanta

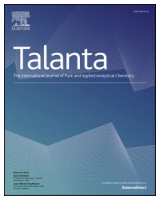

A robust fluorescent glycerol kinase biosensor for reliable quantification of glycerol

Alanna E. Sorenson, Patrick M. Schaeffer *

Biomedical Sciences and Molecular Biology, College of Medicine and Dentistry, James Cook University, Douglas, QLD, 4811, Australia

ARTICLE INFO

Keywords:
Glycerol
ADP
ATP
DSF-GTP
Fluorescent
uvGFP
Glycerol kinase
GlpK
GK-GFP

ABSTRACT

Glycerol is a natural component of many biological samples, beverages and foodstuffs making accurate quantification relevant to a wide variety of industries and applications. Here we present a simple, rapid, and reliable biosensor for quantification of glycerol in a variety of sample types including water, alcoholic beverages, balsamic vinegar, honey, syrup and artificial human urine. This system leverages GFP-tagged *Escherichia coli* glycerol kinase with differential scanning fluorimetry of GFP-tagged proteins for direct quantification of glycerol via binding-induced increases in thermal stability. The GFP tag enables additional indication of potential matrix effects. The biosensor has a broad linear range of 31 μM – 7.5 mM and a limit of detection of 19 μM. Good agreement was obtained between the fluorescent glycerol kinase biosensor and a commercial glycerol quantification kit with glycerol-spiked artificial urine as well as a variety of alcoholic beverages and foodstuffs.

1. Introduction

Glycerol (1,2,3-propanotriol) is a natural component of many biological samples [1] and foodstuffs [2]. In the beverage industries, glycerol contributes to multiple factors including viscosity, softness, and flavour [2–5]. As glycerol is a co-product of ethanol during fermentation the content can be used as an indicator of beverage quality [2,4,5]. Alternatively, adulteration with added glycerol can be used to mask poor quality beverages [6,7]. Adulteration with glycerol is potentially an issue with other foodstuffs such as balsamic vinegar [8]. The presence of glycerol in other foodstuffs such as honey and maple syrup can be an indication of spoilage [9,10] due to fermentation by osmophilic microorganisms.

Determination of glycerol concentration in biological samples such as serum and urine are important for monitoring and diagnosis of various diseases [1]. Serum triglyceride quantification also requires glycerol quantification following lipolysis [11]. In addition, since glycerol is used as a masking agent for doping in competitive sports, oral and intravenous administration of glycerol is prohibited by the World Anti-doping Agency (WADA) [1,12].

Accurate quantification of glycerol is relevant to a wide variety of industries and applications. Various methods have been used to for the quantification of glycerol in a wide range of substances, including chromatographic [8,13–16], spectroscopic [7,17,18], enzymatic [2,4,19–21], titrimetric [3,22,23] and amperometric techniques [1,24–29]. The most widely used techniques are high performance liquid chromatography (HPLC) and gas chromatography (GC) [3]. However, while these techniques are highly sensitive and reproducible they require expensive instrumentation, hazardous solvents, and derivatization of glycerol in the case of GC [1,3]. While titrimetric methods are less expensive, they still require hazardous chemicals [3,23].

Several enzymatic techniques have been developed including a simplified Boehringer Mannheim method [20] and commercial kits employing linked assays. These include combinations of glycerol kinase (GK) and glycerol-3-phosphate oxidase (G3PO) (MAK117, Sigma-Aldrich), GK with pyruvate kinase (PK) and lactate dehydrogenase (LDH) (K-GCROL, Neogen) or GK with ADP-glucokinase (ADP-GK) and glucose-6-phosphate dehydrogenase (G6PDH) (K-GCROLGK, Neogen), coupled with colorimetric, fluorometric or spectroscopic detection of reaction products. While enzymatic methods are sensitive and highly selective, the number of enzymes, cofactors and storage conditions required can increase costs and impact kit stability.

Amperometric methods have also been developed based upon enzymatic reactions, including alcohol dehydrogenase [1], glycerol dehydrogenase (GDH) [24,27,28,30], GK and G3PO [25,26], and GDH and diaphorase [26]. However, despite the high intrinsic selectivity of the enzymes employed, the analytical performance of these amperometric methods can be affected by matrix-related electrochemical

* Corresponding author.
E-mail address: Patrick.schaeffer@jcu.edu.au (P.M. Schaeffer).

https://doi.org/10.1016/j.talanta.2026.130327
Received 4 January 2026; Received in revised form 6 March 2026; Accepted 17 July 2026
Available online 21 July 2026

interference, dissolution of soluble mediators, and the complexity of enzyme immobilization strategies [1]. These limitations highlight the need for enzymatic glycerol sensing strategies that reduce assay complexity while maintaining selectivity and robustness in complex sample matrices.

The GK (P0A6F3) from *Escherichia coli* is a key enzyme in the regulation of glycerol uptake, catalysing the phosphorylation of glycerol via ATP to yield glycerol 3-phosphate (G3P) [31]. Beyond its biological role, GK provides an attractive platform for glycerol sensing due to its high substrate specificity. The enzyme has previously been produced as a green fluorescent protein (GFP) fusion (GK-GFP) for the validation of the GFP-based stability assay (GFP-Basta) [32] and differential scanning fluorimetry of GFP-tagged protein assay (DSF-GTP) [33,34]. DSF-GTP can be performed with any real-time thermal cycler with a FAM/SYBR Green channel to determine the thermal stability of a protein via measurement of the unfolding transition midpoint (T_m) value.

Here, we demonstrate that DSF-GTP can be repurposed as an analytical tool for glycerol determination by exploiting the ligand-induced thermal stabilization of a GK-GFP. In contrast to conventional enzymatic glycerol assays that rely on multi-enzyme reaction cascades and indirect detection of reaction products, the proposed approach directly couples glycerol binding to a thermal shift with fluorescence-based readout within a single enzymatic construct. This design reduces assay complexity and enables internal monitoring of matrix effects through the GFP signal. The system was systematically evaluated and translated into a robust biosensing platform for glycerol quantification, with analytical performance assessed under conditions relevant to complex sample matrices.

2. Materials and methods

2.1. Protein expression and purification

E. coli GK-GFP was expressed in *E. coli* BL21 (DE3)RIPL as previously described [32] using a modified autoinduction Terrific Broth (TB). In a 1 L culture flask, 100 mL TB supplemented with ampicillin (100 μg/mL), chloramphenicol (50 μg/mL), glucose (4 mM) and galactose (0.4 mM) was inoculated with a colony from a freshly grown overnight LB agar plate containing ampicillin and chloramphenicol. The culture was first incubated at 37°C and 250 RPM until log phase, then at 16°C for 72 h. Cell lysis and nickel affinity purification were performed as previously described [33] with minor buffer modifications (i.e. PBS (pH 7.4) was used for lysis and sample loading). The protein fractions were eluted with PBS (pH 7.4) and 250 mM imidazole. GK-GFP was precipitated with ammonium sulphate and resuspended in 50 mM sodium phosphate buffer (pH 7.8) and 2 mM β-mercaptoethanol for storage.

2.2. DSF-GTP with GK-GFP

DSF-GTP was performed in low profile skirted 96-well PCR plates (Bio-Rad) with plate sealing film (Bio-Rad). Reactions were incubated at RT for 5 min prior to melt curve analysis with a Bio-Rad CFX-96. Fluorescence was monitored using the FAM/SYBR Green detection channel. The melt curve protocol included a 2 min equilibration phase at 25°C, followed by a 25-90°C increase (0.5°C increments every 10 s). T_m values were identified using CFX Maestro software (Bio-Rad). The change in thermal stability (ΔT_m) was determined by subtracting the T_m value of the control reaction without ligand from the T_m values of the test reaction with ligand (e.g. glycerol). Apparent binding constants (K_{obs}) were determined as described previously [34,35].

Final test conditions included GK-GFP (1 μM) in buffer A (50 mM sodium phosphate (pH 9)) with or without ligand. Glycerol was tested at 6 mM, 600, 300, 150, 75, 60, 37.5 and 19 μM final concentrations. Serial dilutions of ATP and ADP were tested from 5 to 0.08 mM (final concentrations). Briefly, 25 μL of GK-GFP (2 μM) in 2X buffer A were mixed with 25 μL of ligand solution. Combinations of ligands, i.e. constant glycerol (600 μM final) and variable ATP or ADP, and constant ADP or ATP (500 μM final) with variable glycerol, were also tested. Unless otherwise stated, all reactions were performed in duplicate. Representative results are reported.

2.3. Analytical performance evaluation

Ethanol was included to improve assay robustness and signal reproducibility in matrices containing alcoholic beverages. The optimal ethanol concentration was determined with GK-GFP (1 μM) in buffer B (buffer A + 1 mM ADP) with varying ethanol concentrations (0, 5, 7.5 or 10% (v/v)) and glycerol concentrations in 2-fold dilution series (1.5 mM – 190 μM or 1.2 mM – 150 μM).

The limit of detection (LOD) was determined in buffer C (buffer B + 5% ethanol). For this, 48 tests, each made with 25 μL of GK-GFP (2 μM in 2x buffer C) and 25 μL of glycerol sample (19 μM in reverse osmosis (RO) water) were compared to the same number of controls with RO water. The LOD was determined from the mean T_m value of the RO water controls plus three times the standard deviation.

Similarly, the linear range of GK-GFP was evaluated in Buffer C with 3 overlapping 2-fold dilution series (high, mid and low range) of glycerol in RO water. Glycerol high range dilution series spanned from 120 to 1.9 mM, mid-range from 12 mM to 190 μM and low range from 1.2 mM to 19 μM. Each concentration was tested in duplicate.

2.4. Glycerol concentration determination with GK-GFP

A standard curve was generated for glycerol (2-fold dilution series) from 2 mM to 31 μM (sample concentration). Various sample types were tested including water, urine, red wine, white wine, beer, cider, honey, maple syrup and balsamic vinegar (Table S1). Sample dilution factors were selected to ensure glycerol concentrations fell within the validated linear range of the assay. All samples were diluted in RO water as indicated. Briefly, 25 μL of GK-GFP (2 μM) in 2X buffer C were mixed with 25 μL of diluted sample and the DSF-GTP protocol run. All samples were tested in triplicate.

Spike and recovery evaluations were performed to assess matrix effects and quantitative accuracy with RO water that was spiked with glycerol at 1, 0.5 and 0.1 mM as well as freshly prepared artificial human urine (pH 6.4) [36] that was spiked with glycerol at 3, 2.2 and 1 mM and diluted (1/50) in RO water. Honey was also spiked with additional glycerol to 1 mM, 2 mM and 3 mM.

2.5. Glycerol concentration determination with K-GCROL kit

The same samples tested using GK-GFP were also tested using a commercial glycerol quantification kit (K-GCROL, Neogen Megazyme) using the manual assay format according to manufacturer's instructions. Spiked RO water and artificial urine were tested undiluted. All other samples were diluted in RO water as recommended by the manufacturer. All measurements are reported as mean values, and error bars represent standard deviation unless otherwise stated.

3. Results and discussion

3.1. GK-GFP characterisation

To validate GK-GFP as a suitable device for glycerol determination using DSF-GTP, we first characterized ligand-induced thermal stabilization and apparent binding behaviour under defined buffer conditions. Thorner and Paulus reported a dissociation constant of 10 μM for glycerol and an optimal pH of ~9 for glycerol kinase activity [37], which informed the conditions for this study. DSF-GTP was applied to measure the T_m values of protein unfolding and T_m shifts associated with protein-ligand interactions [33,35,38–40]. Addition of Mg^{2+} ions had no effect on GK-GFP (Fig. S1A). ADP and ATP yielded very similar T_m curve

profiles (Fig. 1A and B) while glycerol clearly induced the largest T_m shifts on GK-GFP in the absence of Mg^{2+} ions (Fig. 1C). Apparent binding constants (K_{obs}) of 3.4 μM (2.5-4.3 μM), 198 μM (111-293 μM) and 206 μM (149-266 μM) were obtained for glycerol, ATP and ADP respectively (Fig. 1D). These experiments establish glycerol as the dominant stabilizing ligand for GK-GFP providing the analytical basis for selective glycerol detection using a DSF-GTP readout. While K_{obs} values are not directly comparable to equilibrium binding constants, differences between ligand binding constants can be proportional [41]. Here, the K_{obs} values were in relatively good agreement with others [31,33,37,42]. Of note, Pettigrew et al. [31] reported dissociation constants of 47 μM for glycerol as well as 110 μM for ATP and 120 μM for ADP at pH 7 in the absence of Mg^{2+} which were similar in the presence of Mg^{2+}.

Next, we evaluated different combinations of ATP or ADP with glycerol in the absence of Mg^{2+} (Fig. 2). In the presence of 500 μM ADP, the T_m of GK-GFP increased progressively with increasing glycerol concentrations, indicating a progressive protein stabilization effect for this combination of ligands (Fig. 2A–C). In stark contrast, in the presence of 500 μM ATP a T_m shift could only be observed with excess glycerol (600 μM) (Fig. 2B and C). At 600 μM glycerol, the T_m of GK-GFP increased moderately with increasing ADP from 130 to 500 μM (Fig. 2D–F). Conversely, T_m values decreased progressively with increasing ATP from 130 to 500 μM (Fig. 2E and F).

The findings indicate that high ATP concentrations in samples could possibly interfere with the GK-GFP system. However, as GK requires Mg^{2+} for ATP-dependent catalysis, omission of Mg^{2+} was expected to prevent glycerol phosphorylation while preserving ligand binding, thereby enabling glycerol detection without enzymatic turnover. Addition of EDTA (1 mM) to GK-GFP with ATP (500 μM) and glycerol (500 μM) yielded near identical T_m values to those obtained with ADP (500 μM) and glycerol (500 μM), suggesting the possible presence of catalytically active divalent metal ions in our protein sample (Fig. S1B). Titration of the protein sample with EDTA in the presence of ATP and glycerol confirmed the presence of divalent metal ions with catalytic activity at an estimated concentration of ~125 μM (Fig. S1C). We suspect that our purification buffer may have contributed to leaching of Ni^{2+} ions from the affinity column. These results indicate that the presence of divalent metal ions could support ATP-dependent catalysis and production of G3P, underscoring the need for stringent metal chelation when applying the GK-GFP system in ATP-rich samples.

However, ATP is not typically present at significant concentrations in urine [43,44], foods or beverages unless microbial contamination and spoilage has occurred [45]. Indeed, ATP is routinely tested to determine food and beverage spoilage [45]. Moreover, G3P is only reported to be inhibitory at limiting glycerol concentrations with a K_i ~2 mM [37] suggesting a limited impact from the presence or production of G3P in samples contaminated with ATP and Mg^{2+}. Most importantly, addition of Mg^{2+} (500 μM), either alone or in combination with excess EDTA (1 mM), had no effect on GK-GFP in the presence of ADP and glycerol demonstrating that the system is unaffected by the presence of divalent cations under these conditions (Fig. S1D). Overall, our results confirm analytically relevant glycerol binding of GK-GFP and the benefits of adding ADP and omitting Mg^{2+} in the assay buffer, thereby minimizing interferences by avoiding conversion of glycerol to G3P while improving detection sensitivity.

3.2. Evaluation of analytical performance

To define assay conditions suitable for real-world sample matrices, we evaluated buffer composition and solvent effects on GK-GFP thermal behaviour and analytical response. Buffer conditions were chosen based upon proximity to the optimal pH reported [37] achievable with our DSF-GTP-compatible buffer (50 mM sodium phosphate) at pH 9.0 and with the aim of enabling glycerol quantification in acidic samples. Our data also demonstrated the beneficial inclusion of ADP which was set to 1 mM to minimize undesirable effects from ATP contaminants. As glycerol quantification in alcoholic beverages was desirable, we examined the effect of ethanol on GK-GFP. Ethanol at 5% (v/v) decreased the GK-GFP T_m values (Fig. 3A) without affecting the ΔT_m values (Fig. S2). Unexpectedly, the overall quality and amplitude of the T_m peaks improved dramatically, especially at lower glycerol concentrations (Fig. 3A). Higher ethanol concentrations (>5%) affected negatively GK-GFP (Fig. S2). Thus, 5% ethanol was found to be ideal to negate the effects of ethanol in alcoholic beverages at appropriate dilutions used for quantification. All subsequent testing was conducted under final conditions of 50 mM sodium phosphate buffer (pH 9.0) with 1 mM ADP and 5% ethanol.

Comparing 48 samples at the theoretical cut-off glycerol concentration (19 μM sample concentration) to an equal number of negative controls yielded significantly different T_m values, with only one control sample overlapping with glycerol samples (Fig. 3B). Based on this statistical separation, a limit of detection of 19 μM glycerol was established under the defined assay conditions. The linear range of the GK-GFP was evaluated with various glycerol dilution series (19-120 μM; 0.19-12 mM;

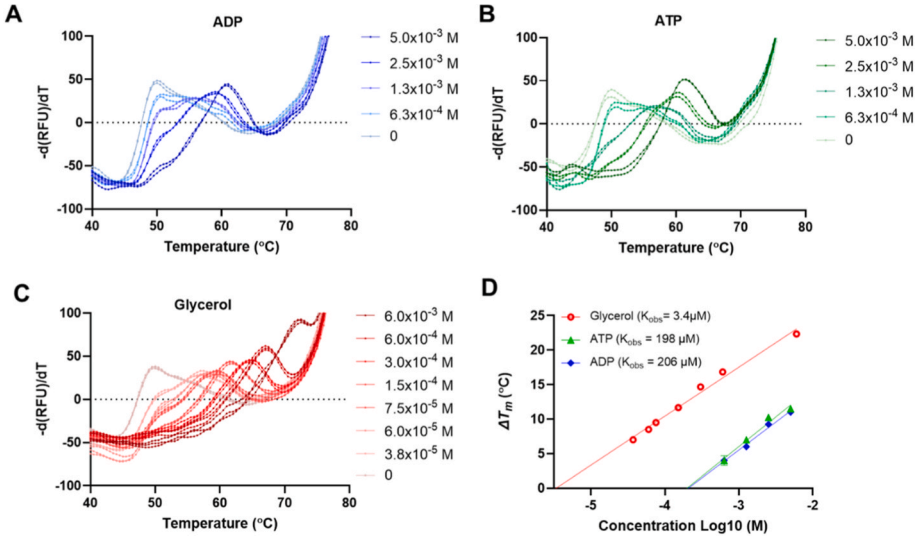

Fig. 1. Effect of ADP, ATP and glycerol on the thermal stability of GK-GFP. DSF-GTP melt curves for GK-GFP (1 μM) in 50 mM sodium phosphate (pH 9.0) with increasing ADP (**A**), ATP (**B**) and glycerol (**C**) concentrations. **D**) ΔT_m values as a function of ligand concentration from datasets (**A-C**) with K_{obs} values determined by linear regression analysis [32,34,38]. n = 2.

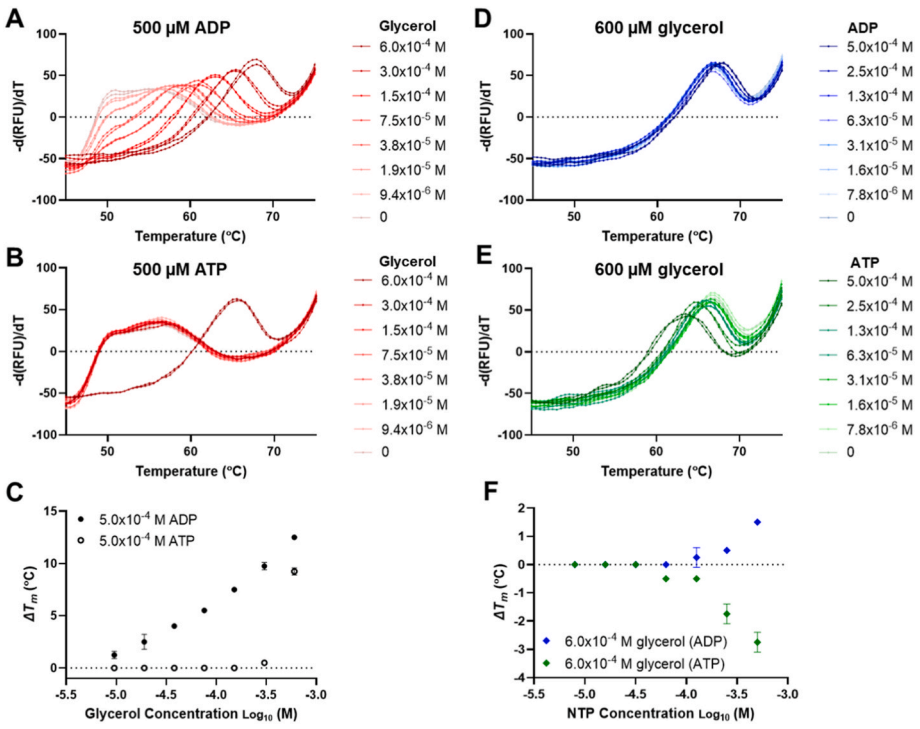

Fig. 2. Effect of ADP, ATP and glycerol combinations on the thermal stability of GK-GFP. Increasing glycerol concentrations on GK-GFP (1 µM) in 50 mM sodium phosphate (pH 9.0) at 500 µM ADP (**A**) and ATP (**B**). **C**) ΔT_m values as a function of glycerol concentration from datasets (**A**) and (**B**). Increasing concentrations of ADP (**D**) and ATP (**E**) on GK-GFP at 600 µM glycerol. **F**) ΔT_m values as a function of ADP or ATP concentration from datasets (**D**) and (**E**). All melt curves (n = 2) were cropped to fit GK T_m range.

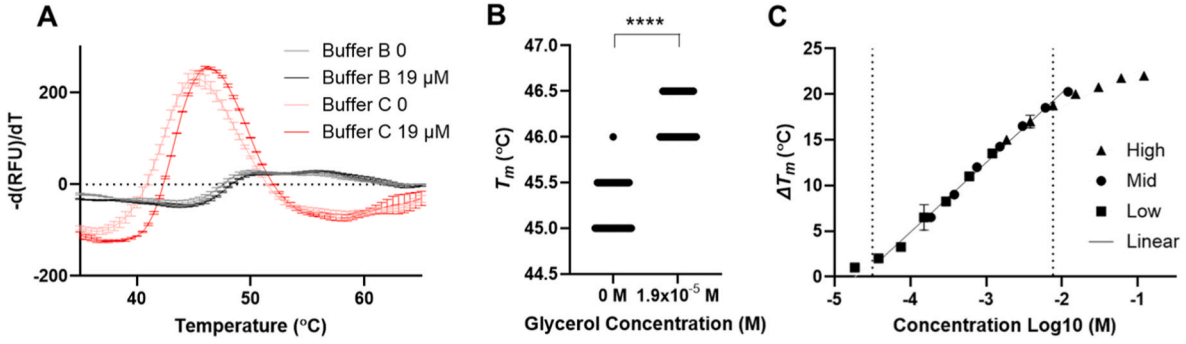

Fig. 3. LOD and linear range of glycerol quantification with GK-GFP. A) GK-GFP (1 µM) melt curves in buffer B (50 mM sodium phosphate (pH 9.0) with 1 mM ADP) and buffer C (buffer B with 5% (v/v) ethanol) with and without 19 µM glycerol (n = 3). **B**) Individual T_m values are shown for GK-GFP with 19 µM glycerol (n = 48) and without glycerol (n = 48) in Buffer C. Statistical analyses performed with Welch's *t*-Test yielded $P < 0.001$ (GraphPad Prism 10). **C**) Linear range was determined in Buffer C with 3 overlapping dilution series (high, mid and low range) of glycerol from 19 µM to 120 mM. Error bars represent SD (n = 2).

1.9-120 mM) demonstrating an effective linear range from 31 µM to 7.5 mM glycerol (Fig. 3C), which is comparable to commercially

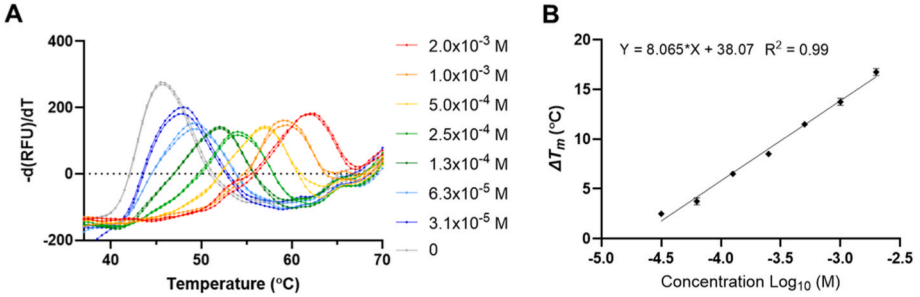

Fig. 4. Standard curve for glycerol quantification using GK-GFP in optimal conditions. A) GK-GFP melt curves obtained for a 2-fold dilution series of glycerol in buffer C (n = 2). **B**) Standard curve for glycerol was fit using linear regression (GraphPad Prism 10).

available kits (Table S2). This range encompasses glycerol concentrations reported in beverages [4,30,46] and exceeds levels relevant for anti-doping screening [47], supporting the suitability of the method for these applications.

3.3. Glycerol detection and applications

To assess quantitative accuracy, matrix tolerance, and real-sample applicability, the GK-GFP DSF-GTP assay was evaluated using spiked standards and diverse sample matrices and benchmarked against a commercial enzymatic kit. First, we generated a standard curve for GK-GFP in RO water (Fig. 4). Next, a glycerol spike and recovery assessment in RO water and artificial urine was performed (Table 1). All spiked samples were tested with GK-GFP and K-GCROL kit. With GK-GFP the recovery ranged from 83 to 114% for RO water and 86-110% for artificial urine. These compared well with the commercial kit recovery values of 107-266% for the same spiked RO water and 102-129% for the artificial urine samples. The greatest discrepancy for both methods occurred at 0.1 mM glycerol, likely due to proximity to the limit of the linear range for each. Additional spike and recovery experiments were performed with the commercial kit's glycerol standard for cross comparison, yielding near identical recoveries (107-109%) (Table 1). The narrower recovery range observed with GK-GFP compared to the commercial kit, particularly at low glycerol concentrations, indicates improved robustness against matrix-dependent signal distortion.

Of note, diluting the artificial urine 50-fold was sufficient to prevent matrix effects. This was determined by testing various 5-fold dilutions of un-spiked artificial urine compared to RO water. At a 10-fold dilution the GK T_m value of GK-GFP decreased by 1.0°C (Fig. S3A) and the amplitude of the GFP T_m peak reduced from 2000 in the RO water control to 1500 in the diluted sample (Fig. S3B). Although the required 50-fold dilution precludes quantification of basal glycerol levels in healthy urine (typically around 17 μM) [48], the assay remains suitable for anti-doping screening, as regulatory thresholds exceed the effective detection limit under these conditions. Thus, GK-GFP would be suitable for the detection of potential blood doping as World Anti-Doping Agency (WADA) regulations state that the glycerol content in urine should not exceed 2.2 mM [47]. Our method could be useful for initial high-throughput screening to identify urine samples requiring further investigation owing to the 96-well format and small sample size required. Of note, our GK-GFP method is easier to perform with a higher throughput and has a similar LOD and broader linear range than a comparable amperometric method for glycerol detection in human urine [1]. Glycerol testing was also trialed in spiked human serum to simulate lipase treatment [49,50]. However, despite heat treatment and clarification via centrifugation, matrix effects were still noticeable with serum diluted 100-fold. As further dilution would prevent useful quantification in sera, this application was abandoned.

A variety of sample types (Table S1) were tested for glycerol content using our GK-GFP method and the commercial K-GCROL kit. Both methods required sample-specific dilution with RO water. In fact, two separate dilutions were performed for each sample type for both methods. In general, GK-GFP required higher sample dilution than the K-GCROL kit to eliminate matrix effects (Table 2). This was primarily required for samples containing tannins and/or with pigmentation (Fig. S3B). Overall, our GK-GFP method compared favorably with previous studies and the K-GCROL kit (Table 2) which is based on an accepted method of the International Organization of Vine and Wine (OIV) and the Central European Brewing Technology Analytical Committee (MEBAK).

A major discrepancy was observed in honey samples. Our GK-GFP data were in agreement with previous studies [19]. In contrast, the higher glycerol concentration measured with the GC-KROL kit may be due to matrix effects from enzymes or pollen, as the manufacturer's guidelines recommend deproteinizing protein-containing samples before analysis. Of note, DSF-GTP can be performed in the presence of protein contaminants [53]. Spiking the honey sample with additional 1-, 2-, and 3-mM glycerol yielded recoveries of 104% ± 3%, 78% ± 9%, and 82% ± 7%, respectively, confirming that our GK-GFP method could accurately detect glycerol in honey.

Maple syrup was not previously shown to contain glycerol [52,54]. Similar concentrations of glycerol were detected with both methods (Table 2), likely indicative of post-production microbial fermentation. Incubation of the diluted maple syrup samples on Luria broth agar resulted in the growth of a near-lawn of slow growing, pink-pigmented bacteria along with several fungal colonies. Partial 16 S rRNA sequencing (See ESI) and BLAST analysis revealed a closest match to the *Methylobacterium* genus, with no hits exceeding 85% identity, and 78% identity to the *Roseomonas* genus. The *Methylobacterium* are known as the Pink-Pigmented Facultative Methylotrophs (PPFMs) and are found ubiquitously in the environment [55], particularly in plant phyllospheres [56]. Although the pink pigmentation is consistent with *Methylobacterium* and *Roseomonas*, the sequence identities suggest this isolate may be a new genus within the family Methylobacteriacea or a distant relative within *Methylobacterium*.

4. Conclusions

The new biosensor system presented here, combining GK-GFP and DSF-GTP, enabled accurate detection and quantification of glycerol in a variety of sample types. Our results were in good agreement with those obtained using a commercial glycerol quantification kit. Yet our method only requires a simple 'mix and run' protocol consisting of combining a neat or diluted sample (1:1) with GK-GFP (2 μM) in 2x Buffer C followed by melt curve analysis in a real-time thermal cycler. A diluted sample volume of 25 μL is sufficient and can be run in 96-well format in ~1 h. In contrast, various reported methods and commercial kits rely on linked reactions requiring multiple steps, enzymes and reagents [21]. As such, our method is also comparatively cost effective especially given that in our hands a 200 mL expression culture yielded GK-GFP (5 mL at 200 μM)

Table 1
Spike and recovery of glycerol in RO water and synthetic urine.

Sample	Spiked glycerol (mM)	GK-GFP DSF-GTP		K-GCROL Kit	
		Found (mM)	% Recovery	Found (mM)	% Recovery
RO water	1.0	1.14 ± 0.07	114 ± 7.5	1.07 ± 0.04	107 ± 3.7
	0.5	0.44 ± 0.00	88 ± 0.0	0.59 ± 0.09	117 ± 19
	0.1	0.083 ± 0.01	83 ± 5.7	0.27 ± 0.06	266 ± 60
Urine[a,b]	3.0	2.59 ± 0.00	86 ± 0.0	3.05 ± 0.67	102 ± 22
	2.2	1.94 ± 0.00	88 ± 0.0	2.27 ± 0.28	104 ± 13
	1.0	1.09 ± 0.00	110 ± 0.0	1.29 ± 0.04	129 ± 3.7
Kit STD	1.0	1.09 ± 0.07	109 ± 7.5	-	-
	1.08	-	-	1.16 ± 0.01	107 ± 0.7

Samples were assayed by adding stock glycerol to yield the intended spike concentration.
[a] Artificial urine was tested diluted 50-fold for GK-GFP and.
[b] undiluted with K-GCROL kit. Recoveries for spiked test samples were calculated by comparison to intended concentrations.

Table 2
Comparison of DSF-GTP and a commercial kit for glycerol quantification in various samples.

Sample	DSF-GTP		K-GCROL		Reported Glycerol Range (mM)Para Run-on	Ref.
	Dilution Factor	Glycerol (mM)	Dilution Factor	Glycerol (mM)		
Red wine	160, 200	160 ± 5.0	160, 200	156 ± 7.4	11-217	[4,30]
White wine	100, 200	75 ± 3.6	100, 200	85 ± 3.7		
Beer	10, 20	19 ± 1.6	5, 10	18 ± 0.9	0.1-22	[46]
Apple Cider	40, 80	63 ± 0.6	10, 20	57 ± 6.0	49-68	[51]
Balsamic vinegar	200, 400	46 ± 15	40, 80	51 ± 0.0	16-87	[8]
Maple syrup	10, 20	15 ± 2.7	10, 20	14 ± 0.1	not detected	[52]
Honey	10, 20	1.8 ± 0.2	10, 20	7.0 ± 2.2	0.5-4	[19]
Spiked Honey (+1 mM)	10	2.8 ± 0.03	N/A	N/A		
Spiked Honey (+2 mM)	10	3.5 ± 0.2	N/A	N/A		
Spiked Honey (+3 mM)	10	4.3 ± 0.2	N/A	N/A		

DSF-GTP testing was performed in triplicate for each dilution. K-GCROL kit testing was performed in duplicate for each sample dilution.

sufficient for ~40,000 tests.

Importantly, the GFP fluorophore not only senses GK unfolding through partial quenching of the fluorescence signal but also serves as an internal quality control measure by reporting on its own unfolding which is affected by matrix effects such as pH. This built-in quality control enables rapid identification of matrix effects in new samples and allows for adjustment of the sample dilution factor as needed. Overall, DSF-GTP with GK-GFP is a reliable method with a broad linear range of 31 μM to 7.5 mM and a LOD of 19 μM for glycerol detection. GK-GFP is compatible with a wide range of sample types and shows potential for high-throughput screening of glycerol in various beverages and food-stuffs for quality control purposes as well as for anti-doping sporting integrity-related urine analysis. It is clear that DSF-GTP will enable the development of other fluorescent biosensors.

CRediT authorship contribution statement

Alanna E. Sorenson: Conceptualization, Formal analysis, Investigation, Methodology, Visualization, Writing – original draft, Writing – review & editing. **Patrick M. Schaeffer:** Conceptualization, Formal analysis, Methodology, Project administration, Visualization, Writing – review & editing.

Declaration of competing interest

The authors declare that they have no known competing financial interests or personal relationships that could have appeared to influence the work reported in this paper.

Appendix A. Supplementary data

Supplementary data to this article can be found online at https://doi.org/10.1016/j.talanta.2026.130327.

Data availability

Data will be made available on request.

References

[1] E. Ramonas, D. Ratautas, M. Dagys, R. Meskys, J. Kulys, Highly sensitive amperometric biosensor based on alcohol dehydrogenase for determination of glycerol in human urine, Talanta 200 (2019) 333–339.
[2] F.C. de Souza, F.J. de Vasconcellos Junior, C. Cabral, T.L. Fernandez, E. D'Elia, Simple enzymatic methods for glycerol analysis in commercial beverages, CyTA - J. Food 11 (3) (2013) 270–276.
[3] L.O. Santos, S.F.L.S. Rocha, C.M. Barra, M. Tubino, J.G. Rocha Junior, Simple, rapid, and reliable titrimetric method for the determination of glycerol at low concentration, J. Braz. Chem. Soc. 33 (6) (2022) 530–540.
[4] I. Popescu-Mitroi, D. Radu, F. Soica, The study of glycerol metabolism in the malolactic fermentation of red wines Romanian Biotechnological letters 19 (1) (2014) 9019–9027.
[5] X. Zhao, S. Procopio, T. Becker, Flavor impacts of glycerol in the processing of yeast fermented beverages: a review, J. Food Sci. Technol. 52 (12) (2015) 7588–7598.
[6] I.S. Pretorius, Tailoring wine yeast for the new millennium: novel approaches to the ancient art of winemaking, Yeast 16 (8) (2000) 675–729.
[7] A.N.S. Cadeado, S.G. Silva, Development of a portable optical device with a multi-channel spectrometer sensor for quantification of glycerol in wine: a maker approach for on-site analysis, Anal Methods-Uk 15 (35) (2023) 4477–4484.
[8] S. Sighinolfi, I. Baneschi, S. Manzini, L. Tassi, L. Dallai, A. Marchetti, Determination of glycerol carbon stable isotope ratio for the characterisation of Italian balsamic vinegars, J. Food Compos. Anal. 69 (2018) 33–38.
[9] M.J. Walker, S. Cowen, K. Gray, P. Hancock, D.T. Burns, Honey authenticity: the opacity of analytical reports - part 1 defining the problem, npj Sci. Food 6 (1) (2022) 11.
[10] S. Bogdanov, P. Martin, Honey authenticity, Mitteilungen aus Lebensmitte-luntersuchung und Hyg 93 (2002) 232–254.
[11] G.R. Warnick, K. Nakajima, Fasting versus nonfasting triglycerides: implications for laboratory measurements, Clin. Chem. 54 (1) (2008) 14–16.
[12] M. Okano, Y. Nishitani, M. Dohi, S. Kageyama, Effects of intravenous infusion of glycerol on blood parameters and urinary glycerol concentrations, Forensic Sci. Int. 262 (2016) 121–127.
[13] H. Li, X. Han, F. Liu, G. Kun-Farkas, Z. Kiss, Simple HPLC method for determining the glycerol content of beer, J. Am. Soc. Brew. Chem. 73 (4) (2018) 314–317.
[14] R.A. Frieler, D.J. Mitteness, M.Y. Golovko, H.M. Gienger, T.A. Rosenberger, Quantitative determination of free glycerol and myo-inositol from plasma and tissue by high-performance liquid chromatography, J. Chromatogr., B: Anal. Technol. Biomed. Life Sci. 877 (29) (2009) 3667–3672.
[15] D.d.A. Cozendey, R.d.O. Muniz, R.C.d. Santos, C.G.d. Souza, D.F.d. Andrade, L. A. d'Avila, Quantitative analysis of free glycerol in biodiesel using solid-phase extraction and high-performance liquid chromatography, Microchem. J. 168 (2021) 106347.
[16] M.C.M. Tabua, W.D. Santiago, M.L. Magalhaes, V.R.F. Ferreira, R.M. Brandao, M. L. Teixeira, M.P. Pedroso, A.M. de Resende Machado, D.L. Nelson, M. das Gracas Cardoso, Identification of volatile compounds, quantification of glycerol and trace elements in distilled spirits produced in Mozambique, J. Food Sci. Technol. 57 (2) (2020) 505–512.
[17] R. Joshi, R. Joshi, H.Z. Amanah, M.A. Faqeerzada, P.K. Jayapal, G. Kim, I. Baek, E.-S. Park, R.E. Masithoh, B.-K. Cho, Quantitative analysis of glycerol concentration in red wine using fourier transform infrared spectroscopy and chemometrics analysis, Kor. J. Anim. Sci. 48 (2) (2021) 299–310.
[18] W. Liang, J. Zuo, Q. Zhou, C. Zhang, Quantitative determination of glycerol concentration in aqueous glycerol solutions by metamaterial-based terahertz spectroscopy, Spectrochim. Acta Mol. Biomol. Spectrosc. 270 (2022) 120812.
[19] J.F. Huidobro, M. Estrella Rea, P.C.B. de Andrade, M. Teresa Sancho, S. Muniategui, J. Simal-Lozano, Enzymatic determination of glycerol in honey, J. Agric. Food Chem. 41 (1993) 557–559.
[20] M.A. Fernandez, M. Teresa Sancho, S. Muniategui, J.F. Huidobro, M.P. Sanchez, J. Simal-Lozano, Direct enzymatic analysis of glycerol in honey: a simplified method, J. Sci. Food Agric. 71 (1996) 141–144.
[21] I. Lapenaite, A. Ramanaviciene, A. Ramanavicius, Current trends in enzymatic determination of glycerol, Crit. Rev. Anal. Chem. 36 (1) (2006) 13–25.
[22] R. Bompelly, D.W. Skaf, Optimization of a colorimetric test method for quantifying glycerol in aqueous solution, J. Am. Oil Chem. Soc. 91 (2014) 1605–1610.
[23] J. Kuhn, H. Muller, D. Salzig, P. Czermak, A rapid method for an offline glycerol determination during microbial fermentation, Electron. J. Biotechnol. 18 (2015) 252–255.
[24] A. Eftekhari, Glycerol biosensor based on glycerol dehydrogenase incorporated into polyaniline modified aluminum electrode using hexacyanoferrte as mediator, Sensor. Actuator. B Chem. 80 (3) (2001) 283–289.
[25] D. Compagnone, M. Esti, M.C. Messia, E. Peluso, G. Palleschi, Development of a biosensor for monitoring of glycerol during alcoholic fermentation, Biosens. Bioelectron. 13 (7–8) (1998) 875–880.
[26] M. Gamella, S. Campuzano, A.J. Reviejo, J.M. Pingarron, Integrated multienzyme electrochemical biosensors for the determination of glycerol in wines, Anal. Chim. Acta 609 (2) (2008) 201–209.

[27] I. Lapenaite, , K. B., L. Marcinkeviciene, I. Bachmatova, V. Laurinavicius, A. Ramanavicius, An enzymatic sensor for the analysis of glycerol in beverages, Chem. Pap. 55 (6) (2001) 345–349.
[28] A. Mahadevan, S. Fernando, An improved glycerol biosensor with an Au-FeS-NAD-glycerol-dehydrogenase anode, Biosens. Bioelectron. 92 (2017) 417–424.
[29] E.V. Zolotukhina, E.V. Butyrskaya, C. Fink-Straube, M. Koch, Y.E. Silina, Towards controlled and simple design of non-enzymatic amperometric sensor for glycerol determination in yeast fermentation medium, Anal. Bioanal. Chem. 416 (15) (2024) 3619–3630.
[30] M. Niculescu, R. Mieliauskiene, V. Laurinavicius, E. Csoregi, Simultaneous detection of ethanol, glucose and glycerol in wines using pyrroloquinoline quinone-dependent dehydrogenases based biosensors, Food Chem. 82 (3) (2003) 481–489.
[31] D.W. Pettigrew, G.J. Yu, Y. Liu, Nucleotide regulation of Escherichia coli glycerol kinase: initial-velocity and substrate binding studies, Biochemistry 29 (37) (1990) 8620–8627.
[32] M.J. Moreau, I. Morin, P.M. Schaeffer, Quantitative determination of protein stability and ligand binding using a green fluorescent protein reporter system, Mol. Biosyst. 6 (7) (2010) 1285–1292.
[33] M.J.J. Moreau, I. Morin, S.P. Askin, A. Cooper, N.J. Moreland, S.G. Vasudevan, P. M. Schaeffer, Rapid determination of protein stability and ligand binding by differential scanning fluorimetry of GFP-tagged proteins, RSC Adv. 2 (31) (2012) 11892–11900.
[34] A.E. Sorenson, P.M. Schaeffer, High-Throughput differential scanning fluorimetry of GFP-Tagged proteins, Methods Mol. Biol. 2089 (2020) 69–85.
[35] T.E.H. Bond, A.E. Sorenson, P.M. Schaeffer, Functional characterisation of Burkholderia pseudomallei biotin protein ligase: a toolkit for anti-melioidosis drug development, Microbiol. Res. 199 (2017) 40–48.
[36] N. Sarigul, F. Korkmaz, I. Kurultak, A new artificial urine protocol to better imitate human urine, Sci. Rep. 9 (1) (2019) 20159.
[37] J.W. Thorner, H. Paulus, Catalytic and allosteric properties of glycerol kinase from Escherichia coli, J. Biol. Chem. 248 (11) (1973) 3922–3932.
[38] M.J. Moreau, P.M. Schaeffer, Dissecting the salt dependence of the Tus-Ter protein-DNA complexes by high-throughput differential scanning fluorimetry of a GFP-tagged Tus, Mol. Biosyst. 9 (12) (2013) 3146–3154.
[39] S. Askin, T.E.H. Bond, P.M. Schaeffer, Green fluorescent protein-based assays for high-throughput functional characterization and ligand-binding studies of biotin protein ligase, Anal Methods-Uk 8 (2016) 418–424.
[40] T.E.H. Bond, A.E. Sorenson, P.M. Schaeffer, A green fluorescent protein-based assay for high-throughput ligand-binding studies of a mycobacterial biotin protein ligase, Microbiol. Res. 205 (2017) 35–39.
[41] D. Matulis, J.K. Kranz, F.R. Salemme, M.J. Todd, Thermodynamic stability of carbonic anhydrase: measurements of binding affinity and stoichiometry using ThermoFluor, Biochemistry 44 (13) (2005) 5258–5266.
[42] S.I. Hayashi, E.C. Lin, Purification and properties of glycerol kinase from Escherichia coli, J. Biol. Chem. 242 (5) (1967) 1030–1035.
[43] Z. Chen, Y. Liu, M. Zhao, S. Zu, Y. Li, B. Shi, S. Wang, X. Zhang, Urinary ATP may be a biomarker for bladder outlet obstruction and its severity in patients with benign prostatic hyperplasia, Transl. Androl. Urol. 9 (2) (2020) 284–294.
[44] K. Gill, H. Horsley, A.S. Kupelian, G. Baio, M. De Iorio, S. Sathiananamoorthy, R. Khasriya, J.L. Rohn, S.S. Wildman, J. Malone-Lee, Urinary ATP as an indicator of infection and inflammation of the urinary tract in patients with lower urinary tract symptoms, BMC Urol. 15 (1) (2015) 7.
[45] M. Bakke, A comprehensive analysis of ATP tests: practical use and recent progress in the total adenylate Test for the effective monitoring of hygiene, J. Food Protect. 85 (7) (2022) 1079–1095.
[46] M. Castellari, E. Sartini, U. Spinabelli, C. Riponi, S. Galassi, Determination of carboxylic acids, carbohydrates, glycerol, ethanol, and 5-HMF in beer by high-performance liquid chromatography and UV-refractive index double detection, J. Chromatogr. Sci. 39 (6) (2001) 235–238.
[47] M. Thevis, S. Guddat, U. Flenker, W. Schanzer, Quantitative analysis of urinary glycerol levels for doping control purposes using gas chromatography-mass spectrometry, Eur. J. Mass Spectrom. 14 (3) (2008) 117–125.
[48] Y. Shen, Z. Xu, An improved GC-MS method in determining glycerol in different types of biological samples, J. Chromatogr., B: Anal. Technol. Biomed. Life Sci. 930 (2013) 36–40.
[49] Y. Chen, Q. Liu, S. Yong, H.L. Teo, T.K. Lee, An improved reference measurement procedure for triglycerides and total glycerides in human serum by isotope dilution gas chromatography-mass spectrometry, Clin. Chim. Acta 428 (2014) 20–25.
[50] C.S. Pundir, V. Narwal, Biosensing methods for determination of triglycerides: a review, Biosens. Bioelectron. 100 (2018) 214–227.
[51] Z. Wang, A. Svyantek, Z. Miller, A.A. Watrelot, Fermentation process effects on fermented McIntosh apple ciders, Fermentation 10 (3) (2024) 115.
[52] A. Saraiva, C. Carrascosa, F. Ramos, D. Raheem, M. Lopes, A. Raposo, Maple syrup: chemical analysis and nutritional profile, health impacts, safety and quality control, and food industry applications, Int. J. Environ. Res. Publ. Health 19 (20) (2022).
[53] S. Askin, T.E.H. Bond, A.E. Sorenson, M.J.J. Moreau, H. Antony, R.A. Davis, P. M. Schaeffer, Selective protein unfolding: a universal mechanism of action for the development of irreversible inhibitors, Chem. Commun. 54 (14) (2018) 1738–1741.
[54] L. Luczaj, M. Bilek, K. Stawarczyk, Sugar content in the sap of birches, hornbeams and maples in southeastern Poland, Cent. Eur. J. Biol. 9 (4) (2014) 410–416.
[55] M.N. Dourado, A.A. Camargo Neves, D.S. Santos, W.L. Araujo, Biotechnological and agronomic potential of endophytic pink-pigmented methylotrophic Methylobacterium spp, Biomed Res. Int. 2015 (2015) 909016.
[56] S. Katayama, K. Shiraishi, K. Kaji, K. Kawabata, N. Tamura, A. Tani, H. Yurimoto, Y. Sakai, Methanol chemoreceptor MtpA- and flagellin protein FliC-dependent methylotaxis contributes to the spatial colonization of PPFM in the phyllosphere, ISME Commun. 5 (1) (2025) ycaf092.